

# Robustness of basal-plane antiferromagnetic order and the $J_{\text{eff}} = 1/2$ state in single-layer iridate spin-orbit Mott insulators

S. Boseggia,<sup>1,2,\*</sup> R. Springell,<sup>3</sup> H. C. Walker,<sup>4</sup> H. M. Rønnow,<sup>5</sup> Ch. Rüegg,<sup>6,7</sup>  
H. Okabe,<sup>8</sup> M. Isobe,<sup>8</sup> R. S. Perry,<sup>9</sup> S. P. Collins,<sup>2</sup> and D. F. McMorrow<sup>1</sup>

<sup>1</sup>*London Centre for Nanotechnology and Department of Physics and Astronomy,  
University College London, London WC1E 6BT, UK*

<sup>2</sup>*Diamond Light Source Ltd, Diamond House, Harwell Science and Innovation Campus, Didcot, Oxfordshire OX11 0DE, UK*

<sup>3</sup>*Royal Commission for the Exhibition of 1851 Research Fellow,  
Interface Analysis Centre, University of Bristol BS2 8BS, UK*

<sup>4</sup>*Deutsches Elektronen-Synchrotron DESY, 22607 Hamburg, Germany*

<sup>5</sup>*Laboratory for Quantum Magnetism, ICMP, École Polytechnique  
Fédérale de Lausanne (EPFL), CH-1015 Lausanne, Switzerland.*

<sup>6</sup>*Laboratory for Neutron Scattering, Paul Scherrer Institut, CH-5232 Villigen PSI, Switzerland.*

<sup>7</sup>*DPMC-MaNEP, University of Geneva, CH-1211 Geneva, Switzerland*

<sup>8</sup>*National Institute for Materials Science (NIMS), 1-1 Namiki, Tsukuba, Ibaraki 305-0044, Japan*

<sup>9</sup>*Scottish Universities Physics Alliance, School of Physics,  
University of Edinburgh, Mayfield Road, Edinburgh EH9 3JZ, Scotland*

(Dated: December 27, 2012)

The magnetic structure and electronic groundstate of the layered perovskite  $\text{Ba}_2\text{IrO}_4$  have been investigated using x-ray resonant magnetic scattering (XRMS). Our results are compared with those for  $\text{Sr}_2\text{IrO}_4$ , for which we provide supplementary data on its magnetic structure. We find that the dominant, long-range antiferromagnetic order is remarkably similar in the two compounds, and that the electronic groundstate in  $\text{Ba}_2\text{IrO}_4$ , deduced from an investigation of the XRMS  $L_3/L_2$  intensity ratio, is consistent with a  $J_{\text{eff}} = 1/2$  description. The robustness of these two key electronic properties to the considerable structural differences between the Ba and Sr analogues is discussed in terms of the enhanced role of the spin-orbit interaction in  $5d$  transition metal oxides.

PACS numbers: 75.25.-j, 71.70.Ej, 75.40.Cx, 78.70.Ck

Transition metal oxides (TMO) containing a  $5d$  element are increasingly attracting attention as an arena in which to search for novel electronic states[1–4]. These are proposed to derive from the strong spin-orbit interaction (SOI) in the  $5d$ 's, which in essence entangles spin and orbital moments, strongly mixing spin and spatial coordinates. Iridium based compounds have featured predominantly in this quest, with considerable focus on the layered perovskites of which  $\text{Sr}_2\text{IrO}_4$  is the prototypical example[5]. In this case, the SOI leads to a  $J_{\text{eff}} = 1/2$  groundstate for the  $\text{Ir}^{4+}$  ( $5d^5$ ) ions, from which a Mott-like insulator then emerges through the action of relatively weak electronic correlations which would otherwise lead to a metallic state. Direct evidence for the existence of a  $J_{\text{eff}} = 1/2$  groundstate in  $\text{Sr}_2\text{IrO}_4$  was provided by x-ray resonant magnetic scattering (XRMS) experiments which revealed a much stronger resonance at the  $L_3$  edge than at the  $L_2$ [6].

The structural similarity of the single-layer iridates to  $\text{La}_2\text{CuO}_4$  adds further impetus to the study of these materials, opening as it does a possible route to the discovery of new families of superconductors[7]. In this context, a particularly interesting compound is  $\text{Ba}_2\text{IrO}_4$ , since structurally it is a closer  $5d$  analogue of  $\text{La}_2\text{CuO}_4$  than the Sr compound.  $\text{Ba}_2\text{IrO}_4$  crystallizes in the  $\text{K}_2\text{NiF}_4$ -type structure (space group  $\text{I}4/\text{mmm}$ ) with  $180^\circ$  Ir-O-Ir bonds in the basal-plane (Fig. 1), and with a 7% tetrag-

onal distortion of the  $\text{IrO}_6$  octahedra along the  $[001]$  direction[8]. In contrast, in  $\text{Sr}_2\text{IrO}_4$  ( $\text{I}4_1/\text{acd}$ ), there is a staggered, correlated rotation of the  $\text{IrO}_6$  octahedra by  $11^\circ$ , and a tetragonal distortion of 4%[9].

From a theoretical point of view, both the tetragonal distortion and the presence or otherwise of octahedral rotations have significant consequences for the electronic and magnetic properties. Firstly, it should be noted that the  $J_{\text{eff}} = 1/2$  state itself is only strictly realized in a system of cubic symmetry[10]. Secondly, the loss of inversion symmetry in  $\text{Sr}_2\text{IrO}_4$  gives rise to a finite Dzyaloshinskii-Moriya (DM) interaction, allowing the formation of non-collinear magnetic structures[11]. Both of these effects on the magnetism in  $\text{Ba}_2\text{IrO}_4$  and  $\text{Sr}_2\text{IrO}_4$  have been investigated using *ab-initio* methods[12].

For  $\text{Sr}_2\text{IrO}_4$ , the consequences of these structural features for the electronic and magnetic properties have been comprehensively explored in a number of experimental and theoretical studies[5, 6, 11, 13]. By contrast, for  $\text{Ba}_2\text{IrO}_4$  there are a number of important open questions, including whether or not its groundstate can reasonably be assigned as  $J_{\text{eff}} = 1/2$ , and the exact nature of its magnetic structure. The latter question is of particular relevance to the prospect of  $\text{Ba}_2\text{IrO}_4$  becoming the parent compound of a new family of unconventional, magnetically mediated superconductors. Both cuprate and pnictide superconductors, for example, emerge when

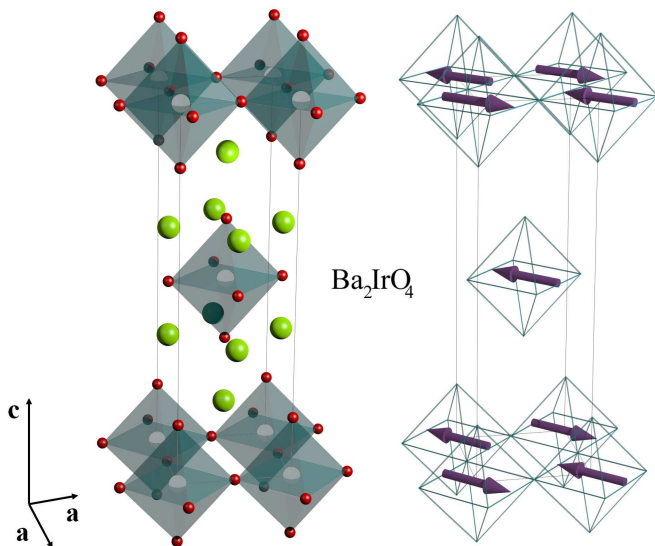


FIG. 1. (Color Online) The left-hand panel shows the crystal structure of Ba<sub>2</sub>IrO<sub>4</sub>. Perovskite IrO<sub>6</sub> layers, where the Ir atoms (grey) lie at the center of corner sharing oxygen (red) octahedra, are separated by Ba atoms (light green). The right-hand panel shows the basal-plane antiferromagnetic structure of the Ba<sub>2</sub>IrO<sub>4</sub> where the magnetic moments are pointing along the [110] direction.

doping destabilizes long-range antiferromagnetic order, and in each case obtaining a microscopic understanding of the magnetic groundstate of the parent compound has played a pivotal role in our knowledge[14, 15]. From a range of bulk probes and muon spin rotation ( $\mu$ SR) it is known that Ba<sub>2</sub>IrO<sub>4</sub> exhibits a magnetic transition below  $\sim 240$  K[8], close to the magnetic transition in Sr<sub>2</sub>IrO<sub>4</sub> of  $T_N \sim 230$  K, below which the magnetic moments in Sr<sub>2</sub>IrO<sub>4</sub> form a canted antiferromagnetic structure[6]. Whether or not the ferromagnetic moment resulting from the canting is inimical for superconductivity when Sr<sub>2</sub>IrO<sub>4</sub> is doped to form a metal is another important open question.

In this letter we report the results of our XRMS investigation of Ba<sub>2</sub>IrO<sub>4</sub>, which addresses both the question of the magnetic structure in Ba<sub>2</sub>IrO<sub>4</sub>, and the relevance of the  $J_{\text{eff}} = 1/2$  description to its electronic groundstate. Our results are compared with corresponding measurements on Sr<sub>2</sub>IrO<sub>4</sub>, for which we also supply supplementary data, and discussed in terms of current theoretical models. The major achievement of our study is to establish that both antiferromagnetic order and the  $J_{\text{eff}} = 1/2$  state are, to a remarkable degree, robust to structural distortions in the single layered iridate perovskites.

Single crystals of Ba<sub>2</sub>IrO<sub>4</sub> were synthesized at the National Institute for Materials Science (NIMS) by the slow-cooling technique under pressure. The sample of size  $\sim 200\mu\text{m} \times 200\mu\text{m} \times 200\mu\text{m}$ , was initially checked with a Supernova x-ray diffractometer using a monochro-

matic Mo source at the Research Complex at Harwell (RCAH), Chilton, UK. The diffraction data are consistent with the  $I4/mmm$  space group and cell parameters  $a=b=4.0223(4)$  Å and  $c=13.301(3)$  Å at room temperature. The Sr<sub>2</sub>IrO<sub>4</sub> single crystals were prepared at the University of Edinburgh following the standard self-flux technique[16]. The correlated rotation of the IrO<sub>6</sub> octahedra about the  $c$  axis reduces the space group symmetry to  $I4_1/acd$ , generating a larger unit cell:  $\sqrt{2}a \times \sqrt{2}b \times 2c$ , under the rotation of the original cell by  $45^\circ$ [9]. The XRMS measurements were performed at the Ir  $L_2$  (12.831 keV) and  $L_3$  (11.217 keV) edges, probing dipolar transitions from  $2p_{3/2}$  to  $5d$  and from  $2p_{3/2}$  to  $5d$ , respectively. The experiment on the Ba<sub>2</sub>IrO<sub>4</sub> crystal was conducted at the I16 beamline of the Diamond Light Source, Didcot, UK. X-rays were focussed to a beam size of  $20 \times 200 \mu\text{m}$  (V  $\times$  H) at the sample position. The sample was mounted in a Displex cryostat with the [110] and [001] directions in the vertical scattering plane. In order to discriminate between different scattering mechanisms, an Au (333) polarization analyzer was exploited for the entire energy range (11.217 keV–12.831 keV). The XRMS study on Sr<sub>2</sub>IrO<sub>4</sub> was performed at the P09 beamline[17] of Petra III, at DESY, Germany. On P09 the x-rays were focused to a beam size of  $50 \times 50 \mu\text{m}$  at the sample position, using a set of focusing mirrors and beryllium compound refractive lenses. The sample was mounted in a Displex cryostat with the [100] and [001] directions in the vertical scattering plane. A pyrolytic graphite (008) crystal was exploited to analyze the polarization of the scattered beam.

In Ba<sub>2</sub>IrO<sub>4</sub>, with the photon energy tuned to be close to the  $L_3$  edge (11.222 keV) and the sample cooled to 50 K, sharp peaks were found at the reciprocal lattice points  $(\frac{1}{2}, \frac{1}{2}, L)$  with  $L$  even. These peaks existed in the rotated photon polarization channel  $\sigma - \pi$  only (see Fig. 2(a)) as expected from the selection rules for XRMS arising from dipolar transitions[18]. We thus deduce that the Ir<sup>4+</sup> magnetic moments order in an antiferromagnetic structure, with a doubling of the unit cell along the in-plane directions, described by a magnetic propagation vector of  $\mathbf{k} = [\frac{1}{2}, \frac{1}{2}, 0]$ .

In Fig. 2(c) we present the energy dependence of the magnetic scattering at  $(\frac{1}{2}, \frac{1}{2}, 8)$  together with x-ray absorption near edge structure (XANES) measurements for energies in the vicinity of the  $L_3$  and  $L_2$  edges. The most notable features of this data are the existence of a well-defined resonance at the  $L_3$  edge, and the complete absence of a response at the  $L_2$  edge within experimental uncertainty. Concerted attempts to find a magnetic response at the  $L_2$  edge by investigating various magnetic reflections all ended in failure. In their study of Sr<sub>2</sub>IrO<sub>4</sub>, Kim *et al.* [6] argued that the observed large XRMS intensity ratio,  $I_{L_3}/I_{L_2}$ , served as a unique fingerprint of the  $J_{\text{eff}} = 1/2$  state, since for the pure  $J_{\text{eff}} = 1/2$  state  $I_{L_2}$  is identically zero. Our results, interpreted in

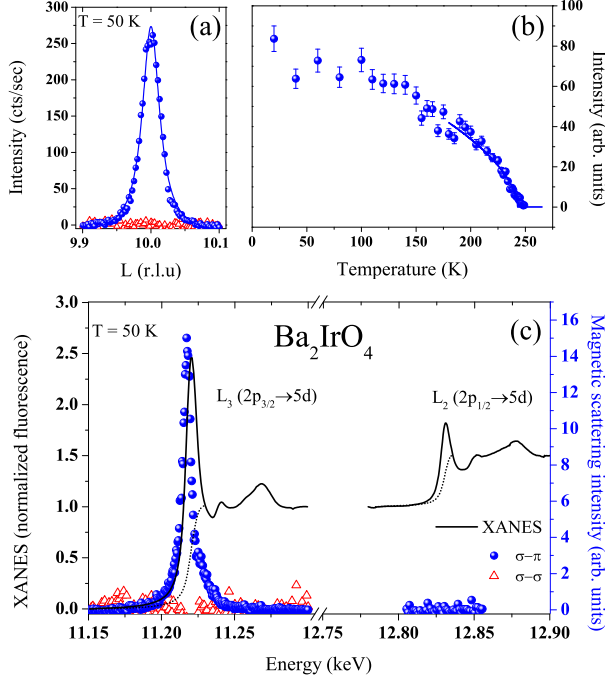


FIG. 2. (Color online) (a)  $L$  scans across the  $(\frac{1}{2} \frac{1}{2} 10)$  magnetic reflection at the Ir  $L_3$  edge,  $T = 50$  K in  $\text{Ba}_2\text{IrO}_4$ . (b) The temperature dependence of the  $(\frac{1}{2} \frac{1}{2} 10)$  magnetic reflection at the Ir  $L_3$  edge in  $\text{Ba}_2\text{IrO}_4$ . The solid blue line is a fit to a power law. (c) Resonant enhancement of the  $(\frac{1}{2} \frac{1}{2} 8)$  magnetic reflection across the  $L_{2,3}$  edges at  $T = 50$  K in  $\text{Ba}_2\text{IrO}_4$ . The solid black line shows the x-ray absorption near edge structure (XANES) spectra, measured in fluorescence mode, normalized to the number of initial states. The blue spheres and red triangles show the intensity of the  $(\frac{1}{2} \frac{1}{2} 8)$  reflection. The black dashed line demarcates the integrated white line used to calculate the branching ratio.

this spirit, establish that even in the presence of a large tetragonal distortion,  $\text{Ba}_2\text{IrO}_4$  belongs to the same class of  $J_{\text{eff}} = 1/2$  spin-orbit Mott insulators as  $\text{Sr}_2\text{IrO}_4$ .

The width of the  $L_3$  resonance is  $\text{FWHM}_{L_3} = 7.6(1)$  eV, comparable to the values found in  $\text{Sr}_2\text{IrO}_4$  and in  $\text{Sr}_3\text{Ir}_2\text{O}_7$ [6, 19]. The position of the resonance, similarly to those of  $\text{Sr}_2\text{IrO}_4$  and  $\text{Sr}_3\text{Ir}_2\text{O}_7$ , is 3 eV below the  $L_3$  white line. From the analysis of the XANES spectra we find a very large branching ratio  $\text{BR} = 5.45$ [20]. This is a further confirmation of the strong SOI regime in  $\text{Ba}_2\text{IrO}_4$ .

The thermal evolution of the antiferromagnetic order was determined by performing  $\theta - 2\theta$  scans of the  $(\frac{1}{2} \frac{1}{2} 10)$  reflection in the  $\sigma - \pi$  channel at the energy (11.219 keV) that maximizes the XRMS response. Fig. 2(b) shows the integrated intensity obtained by fitting a Lorentzian peak shape to the individual scans as a function of temperature. The transition appears to be second order, and from the fit to a  $A(1 - \frac{T}{T_N})^{2\beta}$  function we obtain the Neel temperature  $T_N = 243(1)$  K, in excellent agreement with the value found by  $\mu\text{SR}$  measurements[8].

IR	BV	Atom	BV components					
			$m_{\parallel a}$	$m_{\parallel b}$	$m_{\parallel c}$	$im_{\parallel a}$	$im_{\parallel b}$	$im_{\parallel c}$
$\Gamma_3$	$\psi_1$	1	0	0	1	0	0	0
$\Gamma_5$	$\psi_2$	1	1	1	0	0	0	0
$\Gamma_7$	$\psi_3$	1	1	-1	0	0	0	0

TABLE I. Basis vectors for the space group  $I4/mmm$  with  $\mathbf{k} = [\frac{1}{2} \frac{1}{2} 0]$ . The decomposition of the magnetic representation for the Ir site  $(0, 0, 0)$  is  $\Gamma_{\text{Mag}} = 0\Gamma_1^1 + 0\Gamma_2^1 + 1\Gamma_3^1 + 0\Gamma_4^1 + 1\Gamma_5^1 + 0\Gamma_6^1 + 1\Gamma_7^1 + 0\Gamma_8^1$ . The atom of the primitive basis is defined according to 1:  $(0, 0, 0)$ .

In order to determine the possible magnetic structures in  $\text{Ba}_2\text{IrO}_4$ , we performed representation analysis by means of the *SARAH*[21] package. The input parameters were the system space group  $I4/mmm$ , the magnetic propagation vector  $\mathbf{k} = [\frac{1}{2} \frac{1}{2} 0]$ , resulting from the XRMS measurements, and the atomic coordinates of the Ir atoms. The results of the *SARAH* calculations are presented in Table I. For  $\text{Ba}_2\text{IrO}_4$  only 3 irreducible representations (IR's), with the associated basis vectors, are possible:  $\Gamma_3$ ,  $\Gamma_5$  and  $\Gamma_7$ . Contrary to  $\text{Sr}_2\text{IrO}_4$ , the symmetry of the system, that preserves the inversion symmetry, rules out any representation that involves a ferromagnetic component.

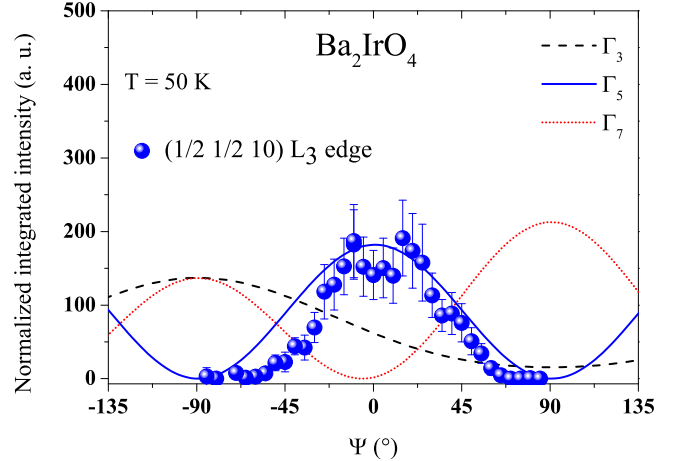


FIG. 3. (Color Online) The azimuthal dependence of the  $(\frac{1}{2} \frac{1}{2} 10)$  magnetic reflection (solid blue spheres) at the Ir  $L_3$  edge,  $T = 50$  K in  $\text{Ba}_2\text{IrO}_4$ . The solid lines are the azimuthal dependencies calculated for the three different IR's. The azimuthal angle  $\Psi$  is defined with respect to the reference vector  $[1 \ 1 \ 0]$  in the  $I4/mmm$  space group.

To discriminate between the 3 possible structures, we performed azimuthal scans of the  $(\frac{1}{2} \frac{1}{2} 10)$  magnetic reflection at the Ir  $L_3$  edge,  $T = 50$  K. This method consists in measuring  $\theta - 2\theta$  scans for different  $\Psi$  angles, rotating the sample around the scattering vector. From the azimuthal modulation of the intensity of the XRMS

signal it is possible to determine the orientation of the magnetic moments in an antiferromagnetic material[22]. Fig.3 shows the azimuthal dependence of the  $(\frac{1}{2} \frac{1}{2} 10)$  reflection (blue solid points). The dashed black line, solid blue line and dotted red line are the azimuthal dependence for the  $\Gamma_3$ ,  $\Gamma_5$  and  $\Gamma_7$  IR, respectively, calculated by means of the FDMNES package[23]. The experimental curve most closely resembles the calculation for the  $\Gamma_5$  representation. We therefore conclude unambiguously that  $\text{Ba}_2\text{IrO}_4$  exhibits a basal-plane antiferromagnetic order with the magnetic moments pointing along the  $[110]$  direction. The magnetic structure of  $\text{Ba}_2\text{IrO}_4$  is shown in Fig. 1.

To understand the dependence of the  $J_{\text{eff}} = 1/2$  state and the associated Hamiltonian on symmetry and lattice distortions, we have investigated the magnetic structure of  $\text{Sr}_2\text{IrO}_4$ . In particular we focus on the polarization and azimuthal dependencies of the XRMS, neither of which have been reported[6]. With the photon energy tuned to the Ir  $L_3$  edge, well defined magnetic peaks were found at the  $(104n)$  and  $(014n+2)$  Bragg positions, which are forbidden within the  $I4_1/acd$  space group and correspond to the  $(\frac{1}{2} \frac{1}{2} L)$  peaks observed in the  $\text{Ba}_2\text{IrO}_4$  (as illustrated in the inset of Fig. 4(c)). Fig. 4(a-b) shows the  $L$  scan and the energy scan of the  $(1024)$  magnetic reflection at the Ir  $L_3$  edge at  $T=90$  K. The well defined  $L$  scan supports the existence of a long-ranged antiferromagnetic order. The Lorentzian shape of the energy scan ( $\text{FWHM}_{L_3} = 6.26(9)$  eV) and the absence of any  $\sigma - \sigma$  scattering mechanism confirms the magnetic nature of the peaks, similarly to  $\text{Ba}_2\text{IrO}_4$ . These results are in agreement with the first XRMS study of  $\text{Sr}_2\text{IrO}_4$  [6].

In order to determine the direction of the magnetic moments in  $\text{Sr}_2\text{IrO}_4$  we performed azimuthal scans at the Ir  $L_3$  edge,  $T = 90$  K. The results, together with the FDMNES calculation using the same moment direction as in the irreducible representation  $\Gamma_5$  of  $\text{Ba}_2\text{IrO}_4$ , are presented in Fig. 4(c). Note the equivalence of the  $\Psi$  angles in Fig. 4 with those in Fig. 3, for the correspondence of the  $[110]$  direction in  $I4/mmm$  to the  $[100]$  direction in the  $I4_1/acd$ . By comparing the azimuthal dependence of the  $(1024)$  reflection in  $\text{Sr}_2\text{IrO}_4$  with the azimuthal dependence of  $(\frac{1}{2} \frac{1}{2} 10)$  reflection in  $\text{Ba}_2\text{IrO}_4$ , we deduce that in  $\text{Sr}_2\text{IrO}_4$  the antiferromagnetic component is oriented along the  $[110]$  direction of the  $I4/mmm$  reference system. We therefore conclude that the two compounds have essentially the same basal-plane antiferromagnetic structure[24].

We now turn to the discussion of our results. An effective, low-energy Hamiltonian for the layered iridates, valid in the strong SOI limit, incorporating both the effects of a tetragonal crystal field and rotation of the  $\text{IrO}_6$  octahedra (by an angle  $\alpha$ ), has been derived by Jackeli and Khaliullin [11], which we write as

$$\mathcal{H}_{ij} = J\vec{S}_i \cdot \vec{S}_j + J_z S_i^z S_j^z + D \cdot [\vec{S}_i \times \vec{S}_j] + \mathcal{H}'. \quad (1)$$

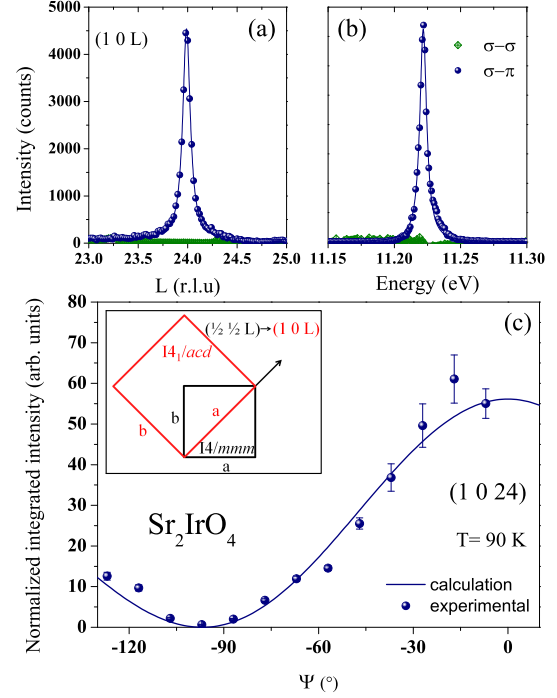


FIG. 4. (Color Online) Reciprocal space  $L$ -scan (a) and energy dependence (b) of the XRMS intensity of the  $(1024)$  reflection in  $\text{Sr}_2\text{IrO}_4$  at the Ir  $L_3$  edge,  $T = 90$  K. The solid blue line is a fit to a Lorentzian peak shape. The azimuthal dependence of the same reflection (c) is compared with a calculation for collinear moments along  $[100]$ . The azimuthal angle  $\Psi$  is defined with respect to the reference vector  $[100]$  in  $I4_1/acd$ , which corresponds to the  $[110]$  in the  $I4/mmm$  space group, as demonstrated in the inset by means of a 2D projection onto the basal-plane of the unit cell.

The terms on the righthand side are the isotropic Heisenberg exchange, the symmetric and asymmetric DM anisotropies, and finally an anisotropic contribution from the Hund's coupling[11]. This Hamiltonian has been used to successfully account for the canted magnetic structure observed in  $\text{Sr}_2\text{IrO}_4$  [6], and additionally for a dimensionally driven spin reorientation in its bi-layer counterpart  $\text{Sr}_3\text{Ir}_2\text{O}_7$ [19, 22, 25]. For  $\text{Ba}_2\text{IrO}_4$ , it would also seem to offer a natural explanation of our results: with  $\alpha=0$ , the second and third terms are identically zero, leaving a leading isotropic exchange along with a weaker anisotropy, a Hamiltonian that readily supports the commensurate antiferromagnetic order observed in our experiments. One important proviso, however, is that the magnetic groundstate supported by this Hamiltonian becomes unstable above a critical value of tetragonal distortion leading to a spin reorientation where the moments point along the  $[001]$  direction. Nevertheless it seems, that nearly doubling the tetragonal distortion in moving from Sr to Ba is insufficient to exceed the critical threshold.



Although the above analysis provides a general framework for us to understand the formation of magnetic structures in the layered perovskites, and most especially the canting of the moments in  $\text{Sr}_2\text{IrO}_4$ , it does not address the key fact revealed in our experiments that the antiferromagnetic components in the two compounds are essentially identical. For this we refer to explicit calculations of  $J$  by Katukuri *et al.* [12], who used an *ab-initio* many-body approach. Their calculations show that when the SOC is switched off, the groundstate and the magnetic interactions are extremely sensitive to the local symmetry and so very different in the two systems:  $\text{Ba}_2\text{IrO}_4$  has a hole in the  $d_{xz}/d_{yz}$  states and a strong antiferromagnetic  $J$  interaction ( $\sim 15.4$  meV),  $\text{Sr}_2\text{IrO}_4$  has a hole in the  $d_{xy}$  state and a ferromagnetic  $J$  interaction ( $\sim -19.2$  meV). However, upon including the SOC, the hole acquires an equal  $d_{xy}$ ,  $d_{zx}$  and  $d_{yz}$  character in both compounds and  $J$  in  $\text{Sr}_2\text{IrO}_4$  becomes antiferromagnetic ( $\sim 51.3$  meV), and almost identical to that in  $\text{Ba}_2\text{IrO}_4$  ( $\sim 58$  meV). Therefore, the robustness of antiferromagnetic order in the layered perovskites to structural distortions, is ultimately linked to the strong SOI, which produces a groundstate wavefunction that is three dimensional and inherently less perturbed by structural distortions.

In this letter we have presented a detailed XRMS study of the magnetic and electronic structures of the single layered iridates  $\text{Ba}_2\text{IrO}_4$  and  $\text{Sr}_2\text{IrO}_4$ .  $\text{Ba}_2\text{IrO}_4$  is found to be a basal-plane commensurate antiferromagnet below  $T_N = 243$  K. Azimuthal scans combined with group theory calculations have been employed to prove that the moments order along the  $[110]$  direction. From a comparison with XRMS data on the related compound  $\text{Sr}_2\text{IrO}_4$ , we establish that both compounds have essentially the same basal-plane antiferromagnetic structure, in spite of their structural differences. We also conclude from our results for the intensity ratio  $L_3/L_2$  of the XRMS signal that  $\text{Ba}_2\text{IrO}_4$  is also in the same class of  $J_{\text{eff}} = 1/2$  spin-orbit Mott insulators as  $\text{Sr}_2\text{IrO}_4$ . Thus both the magnetic and electronic structures in the layered perovskites are remarkably robust to structural distortions, a fact that can be linked directly to the unique three-dimensional character of the  $J_{\text{eff}} = 1/2$  state produced by the strong SOI which renders it insensitive to the perturbations in local symmetry.

We would like to thank the Impact studentship programme, awarded jointly by UCL and Diamond Light Source for funding the thesis work of S. Boseggia. G. Nisbet provided excellent instrument support and advice on multiple scattering at the I16 beamline. We also thank J. Strempler and D. K. Shukla for technical support at P09. The research was supported by the EPSRC, and part of the research leading to these results has received funding from the European Community's Seventh Framework Programme (FP7/2007-2013) under grant agreement n° 312284.

- 
- \* stefano.boseggia@diamond.ac.uk
- [1] D. Pesin and L. Balents, *Nat Phys* **6**, 376 (2010).
  - [2] X. Wan, A. M. Turner, A. Vishwanath, and S. Y. Savrasov, *Phys. Rev. B* **83**, 205101 (2011).
  - [3] J. Chaloupka, G. Jackeli, and G. Khaliullin, *Phys. Rev. Lett.* **105**, 027204 (2010).
  - [4] W. Witczak-Krempa and Y. B. Kim, *Phys. Rev. B* **85**, 045124 (2012).
  - [5] B. J. Kim, H. Jin, S. J. Moon, J.-Y. Kim, B.-G. Park, C. S. Leem, J. Yu, T. W. Noh, C. Kim, S.-J. Oh, J.-H. Park, V. Durairaj, G. Cao, and E. Rotenberg, *Phys. Rev. Lett.* **101**, 076402 (2008).
  - [6] B. J. Kim, H. Ohsumi, T. Komesu, S. Sakai, T. Morita, H. Takagi, and T. Arima, *Science* **323**, 1329 (2009).
  - [7] F. Wang and T. Senthil, *Phys. Rev. Lett.* **106**, 136402 (2011).
  - [8] H. Okabe, M. Isobe, E. Takayama-Muromachi, A. Koda, S. Takeshita, M. Hiraishi, M. Miyazaki, R. Kadono, Y. Miyake, and J. Akimitsu, *Phys. Rev. B* **83**, 155118 (2011).
  - [9] M. K. Crawford, M. A. Subramanian, R. L. Harlow, J. A. Fernandez-Baca, Z. R. Wang, and D. C. Johnston, *Phys. Rev. B* **49**, 9198 (1994).
  - [10] A. Abragam and B. Bleaney, *Electron paramagnetic resonance of transition ions*, International series of monographs on physics (Clarendon P., 1970).
  - [11] G. Jackeli and G. Khaliullin, *Phys. Rev. Lett.* **102**, 017205 (2009).
  - [12] V. M. Katukuri, H. Stoll, J. van den Brink, and L. Hozoi, *Phys. Rev. B* **85**, 220402 (2012).
  - [13] S. Fujiyama, H. Ohsumi, T. Komesu, J. Matsuno, B. J. Kim, M. Takata, T. Arima, and H. Takagi, *Phys. Rev. Lett.* **108**, 247212 (2012).
  - [14] P. A. Lee, N. Nagaosa, and X.-G. Wen, *Rev. Mod. Phys.* **78**, 17 (2006).
  - [15] J. Zhao, Q. Huang, C. de la Cruz, S. Li, J. W. Lynn, Y. Chen, M. a. Green, G. F. Chen, G. Li, Z. Li, J. L. Luo, N. L. Wang, and P. Dai, *Nature materials* **7**, 953 (2008).
  - [16] G. Cao, J. Bolivar, S. McCall, J. E. Crow, and R. P. Guertin, *Phys. Rev. B* **57**, R11039 (1998).
  - [17] J. Strempler *et al.*, (to be submitted to *J. Synch. Rad.*).
  - [18] J. P. Hill and D. F. McMorrow, *Acta Crystallographica Section A* **52**, 236 (1996).
  - [19] S. Boseggia, R. Springell, H. C. Walker, A. T. Boothroyd, D. Prabhakaran, D. Wermelle, L. Bouchenoire, S. P. Collins, and D. F. McMorrow, *Phys. Rev. B* **85**, 184432 (2012).
  - [20] For a more detailed analysis of the branching ratio in  $\text{Ba}_2\text{IrO}_4$  see Supplemental Material.
  - [21] A. Wills, *Physica B: Condensed Matter* **276278**, 680 (2000).
  - [22] S. Boseggia, R. Springell, H. C. Walker, A. T. Boothroyd, D. Prabhakaran, S. P. Collins, and D. F. McMorrow, *Journal of Physics: Condensed Matter* **24**, 312202 (2012).
  - [23] Y. Joly, *Phys. Rev. B* **63**, 125120 (2001).
  - [24] We note that XRMS does not couple to a canted component since the latter can be seen as a ferromagnetic modulation of the antiferromagnetic structure. As a consequence, this scattering mechanism occurs in the same position in the reciprocal lattice as the charge scattering.
  - [25] J. W. Kim, Y. Choi, J. Kim, J. F. Mitchell, G. Jackeli, M. Daghofer, J. van den Brink, G. Khaliullin, and B. J.

Kim, Phys. Rev. Lett. **109**, 037204 (2012).